

Characterization of Solid Materials for Terahertz Standoff Detection.

PI: S. James Allen, Physics Dept. UCSB
805-893-7134
allen@iqcd.ucsb.edu

Contract Period: 23 August 2005 – 30 September 2005.

Objective: To obtain preliminary data that will help make an early identification of opportunities, obstacles, and critical issues that need attention for standoff detection of high explosives by terahertz spectroscopic imaging.

Accomplishments:

- Measured reflectance spectra from 500 GHz to 3THz of K-9 training material.
- Measured the broad band reflectance spectra of a cyanuric acid pressed pellet simulant
- Measured angle dependent scattering of coherent radiation from the UCSB free-electron lasers from the pressed pellet simulant.
- Measured the transmission of terahertz radiation through various fiber material that would mask high explosives.

Conclusions:

- Dilute mixtures of high explosives (like K-9 training material) are not useful for developing a detailed catalog of terahertz reflectance signatures.
- Material like cotton absorb strongly as the frequency rises above 1 THz. Spectroscopic imaging through clothing will be most effective below 1 THz and unlikely above 2 THz.
- Below 1 THz the ratio of specular to diffuse scattering will be very sensitive to surface texture.

Contents

Terahertz Reflectance Spectra	2
Cyanuric acid	2
Pressed pellet.	2
Sand matrix	3
RDX, TNT and PETN	4
RDX/Sand.....	5
RDX/Vaseline.....	5
Specular/Diffuse Reflection from Simulant	6
Low angular resolution at 660 GHz.....	6
Near normal reflectance 600GHz, at the diffraction limit.....	8
Transmission through the Simulant	9
Terahertz Transmission through Various Materials	10
Atmospheric water.....	10
Miscellaneous fiber materials, some clothing related.....	10

Terahertz Reflectance Spectra

Terahertz spectral reflectance measurements were performed with a Bruker IFS66-V Fourier transform infrared (FTIR) spectrometer, married to a QMC cryogenic composite bolometer. It is an evacuated instrument, free of water vapor absorption. A stage was designed and fabricated at UCSB to make near normal reflectance measurements while providing the high throughput required to get good signal to noise at the longest wavelengths. (See Fig. 1.)

The radiation was not polarized. The angle of incidence was approximately $\sim 10^\circ$. In most cases the reflectivity from the material under test was very low and typically $< .05$. Under these conditions it was important to judiciously place THz absorber in the sample compartment to mitigate any radiation that might reach the detector without being reflected by the test sample.

Materials examined were the following.

- A pressed composite consisting of 45% cyanuric acid, 44.5% talc and 10.5% polyisobutylmethacrylate.
- 8% Cyanuric acid in sand
- K-9 training materials consisting of 8% concentrations of RDX, PETN and TNT in sand and Vaseline.

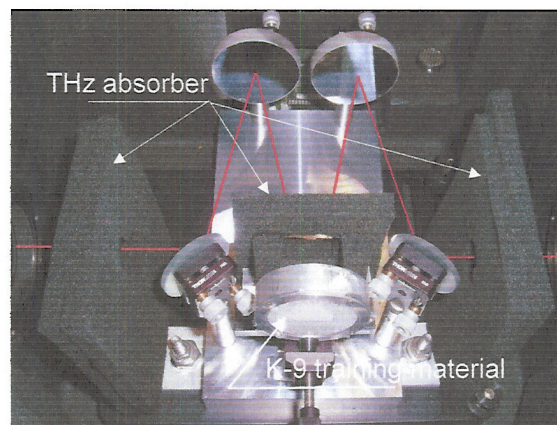


Fig. 1 Reflection rig for the Bruker IFS66V FTIR. Absorber minimizes contamination by spurious reflections.

Cyanuric acid

Pressed pellet.

To simulate the mechanical properties, and perhaps the dielectric properties, of solid high explosive targets, pressed pellets were fabricated at LLNL and delivered to UCSB. They consisted of a physical mixture of 45% cyanuric acid,

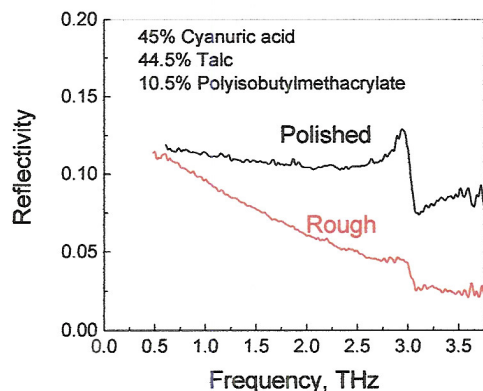


Fig. 2 Reflectivity from polished and belt sanded surfaces of cyanuric acid simulant



Fig. 3 Pressed cyanuric acid pellet.

44.5% talc and 10.5% polyisobutylmethacrylate. They were approximately 50 mm in diameter and 6 mm thick and presented four different surface textures. One polished, two roughened by a belt sander the fourth smooth but not polished. Work focused on the two extremes – the polished surface and a surface roughened on a belt sander. The pellet is shown in Fig. 3.

Reflectivity from the polished and roughened surfaces is shown in Fig. 2. Of particular note is the strong resonance around 3 THz. Reflectance spectra are expected to emphasize the real part of the dielectric constant and the line shape shown is consistent with this interpretation. Identification with the cyanuric acid component is brought forward only after recovering a similar feature in the 8% cyanuric acid/sand mixture. We may conclude that reflectance spectra of physical mixtures can present relatively sharp features in this part of the electromagnetic spectrum, but with the dispersive line shape shown in Fig. 1.

Near ~ 600 GHz the reflectance is in rough agreement with estimates of normal reflectivity extracted with the coherent radiation from the FEL. The broad band spectra in Fig. 2 show little effect of surface roughness at ~ 600 GHz. But it is also apparent that at higher frequencies surface texture does begin to diminish the specular reflectivity. (Presumably there is more diffuse scattering.) Quantitative measures of surface roughness and frequency dependent diffuse scattering are called for here but were not performed in the contract period. (23 August – 30 September.)

Sand matrix

Knowing that the high explosive materials (RDX, TNT and PETN) were only available as an 8% physical mixture in sand and vaseline, experiments were carried out on 8% cyanuric acid in sand. Comparison of the relatively dilute sand mixture to the more concentrated pressed pellet may allow some perspective on the utility of using K-9 training samples to develop fingerprinting spectra.

Sample holders consisted of aluminum rings with thin film windows on front and back. The sand (or vaseline) mixture was loaded into the cell between the windows and the reflectivity of the thin film / sand mixture was measured as was done for the composite pellet. The thin film windows in the early sample holders fabricated at LLNL were $\sim 50 \mu\text{m}$ polypropylene glued to an aluminum frame. As the work preceded it was apparent that, with the very low reflectivity from the sand, the signal was dominated by reflectivity from the polypropylene windows. This was largely mitigated by fabricating new holders at UCSB that could support $2.5 \mu\text{m}$ mylar windows. (See Fig. 4.)

Reflectivity of sand and the sand cyanuric acid mixture is shown in Fig. 5. The overall frequency dependent reflectivity, peaking at ~ 2 THz (Fig. 5 b), exhibited with the LLNL sample holders, most likely reflects a thin film Fabry-Perot etalon effect in the polypropylene window. Indeed, replacing the widow with much thinner, $2.5 \mu\text{m}$, mylar moves this broad etalon

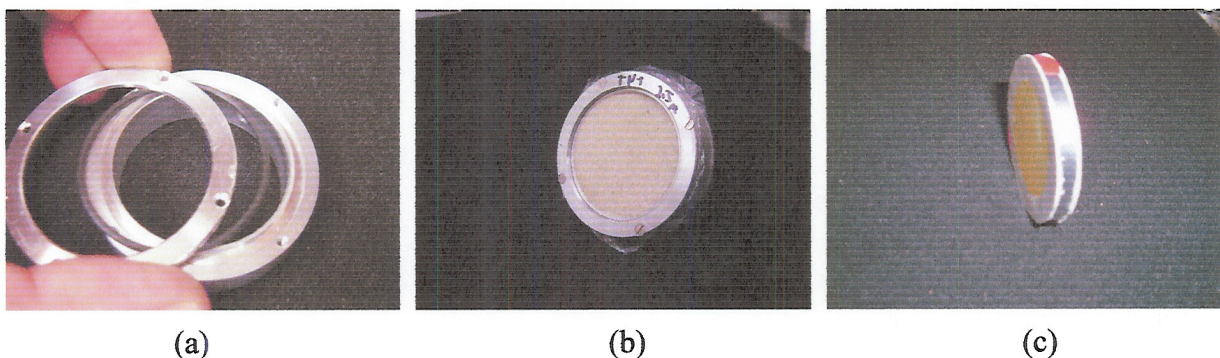


Fig. 4 Sample holders for sand or vaseline mixtures. (a) Retainer and o-ring design that pulls a tight $2.5 \mu\text{m}$ window across the frame. (b) same as (a) with a TNT sand mixture in place. (c) LLNL frame with $50 \mu\text{m}$ polypropylene window glued to aluminum frame.

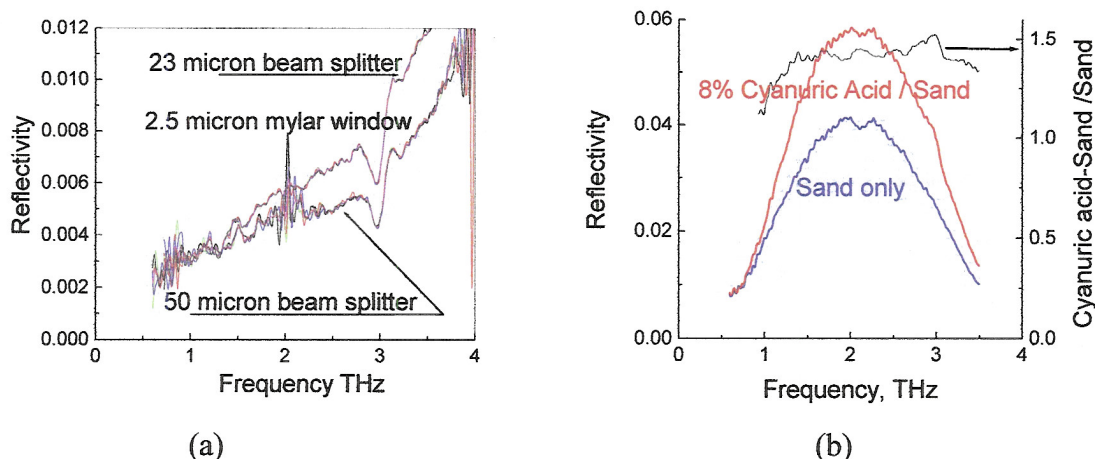


Fig. 5 (a) Reflectivity of 8% cyanuric acid mixture with 2.5 micron mylar window. (b) The same but with the LLNL sample holder and 50 micron polypropylene window. Note that the reflectivity scale in (a) is 5 times smaller.

resonance to much higher frequencies and out of the range of interest (Fig. 5 a). The *specular* reflectivity from the sand is very low indeed. The rising reflectivity shown in Fig. 5 a is probably residual reflectivity from the thin window, yet the composite reflectivity reveals what we identify as the cyanuric acid resonance ~ 3 THz.

While we may take some satisfaction from “teasing” out of the reflectance spectra the strong signature for cyanuric acid at ~ 3 THz, K-9 training samples are not an effective or productive way to develop a catalog of spectral reflectance signatures for high explosive targets. A program, with all the safety protocols, that can extract measurements like those performed on the pressed cyanuric acid pellet but on real high explosive material is essential.

RDX, TNT and PETN

RDX, TNT and PETN were only available as K-9 training samples with 8% physical mixtures in sand and vaseline. Under these circumstances and in the light of the results with the cyanuric acid, work was essentially guided by published data on these materials, recovering data in the mixtures that was consistent with known spectra. Data on transmission through the atmosphere and clothing suggests that a potential stand-off spectral imaging system will work best at the low end of the terahertz spectrum. From this perspective, most of the effort focused on RDX since it presents a feature below ~ 1 THz. See Table 1.

Material	Frequency, THz
RDX	0.8 2.4
TNT	1.7
PETN	2.0 2.7

Table 1 THz spectral signatures measured in transmission and documented by Cook et al. Physical Sciences Inc.

<http://www.psicorp.com/publications/PDF/VG03-077.pdf>

RDX/Sand

Knowing that RDX has an absorption feature at ~ 800 GHz, one can identify a feature in reflection from the RDX/sand mixture that may be due to the RDX. (Fig. 6) As noted earlier, the specular reflectivity of the sand itself is very low. Without foreknowledge of the RDX absorption spectra, we would be hard pressed to conclude, based on Fig. 6, that there is RDX present.

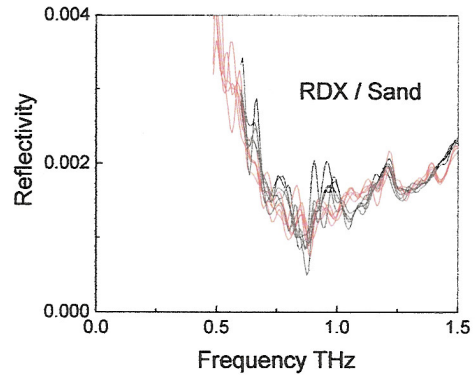


Fig. 6 Reflectivity of RDX/sand mixture focused on the region where a feature is expected, ~ 800GHz.

RDX/Vaseline

Reflection spectra for RDX/Vaseline mixtures present more convincing data. (Fig. 7) Two features, 800 GHz and ~ 2.0 THz, appear to correlate with known resonances in RDX. Note that the overall specular reflectivity is much higher for Vaseline than sand.

Lastly, the reflectivity of the RDX/Vaseline mixture was measured with the sample draped with cotton. (See Fig. 17 to understand the transmission characteristics of the cotton.) The cotton transmission is falling rapidly at these frequencies and the weak reflection feature at ~ 800 GHz can be seen but only with some forehand knowledge. (Fig. 8)

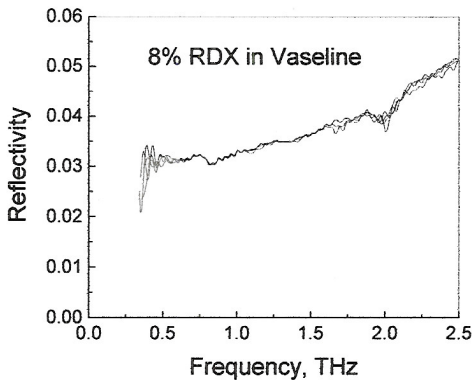


Fig. 7 Reflectivity of RDX/Vaseline mixture exhibiting two resonances that appear to correlate with known features in RDX.

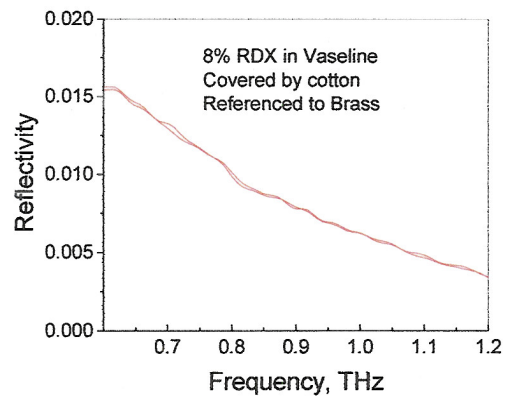


Fig. 8 Reflectivity of the same sample in Fig. 7 draped with cotton. See Fig. 17.

Specular/Diffuse Reflection from Simulant

Angle resolved reflectivity from the pressed pellet used for the broad band FTIR measurements were recovered with coherent radiation from the UCSB free-electron lasers. (~ 45% cyanuric acid, ~ 44.5% talc, 10.5% polyisobutylmethacrylate) The pellets were ~ 50 mm in diameter and ~ 6 mm thick. The pellets presented 4 different textures. At the extremes one presented a polished surface while another a surface roughened with a belt sander. The data recovered with the free-electron lasers at 600 and 660 GHz indicates that the reflection is essentially specular for both surfaces. Measurements with the FTIR at near normal incidence are consistent with the FEL results at ~ 600 GHz and indicate that the surface roughness is important only above ~ 1 THz. To the extent that the simulant mimics the dielectric, microstructure and surface texture of potential targets one would conclude that the reflected radiation below 1 THz will be specular. Of course surface texture with larger scale, presumably comparable to and greater than the wavelengths of interest would result in larger diffuse components and completely different conclusions.

Two sets of experiments were carried out;

- relatively low angular resolution (~5 degrees),
- diffraction limited resolution at ~600 GHz, 0.5 mm wavelength.

Low angular resolution at 660 GHz.

Fig. 9 shows the apparatus that was used to measure radiation reflected from the sample as a function of take off angle. The incident angle could also be adjusted and here it is set at ~ 45 degrees. The bolometric detector “rolls” around the sample and detects the reflected power. The polarization of the incident radiation is set as s or p. (S polarized radiation orients the electric vector so as to be parallel to the surface at any angle of incidence. The electric vector for p polarization is in the plane of incidence.)

Fig. 10 exhibits the angular dependence of the radiation reflected at 45° from a 1st surface mirror used to normalize the measurements on the simulant. It indicates that the instrument resolution was about 5° full width at 1/2 maximum.

Only data from the roughest surface (belt sanded) was recovered, as we focused on the effects of surface roughness. For the roughest surface, finished or roughened with a belt sander, the striations were oriented perpendicular or parallel to the plane of incidence. (After the fact, we learned that at these frequencies the roughness was not significant.)

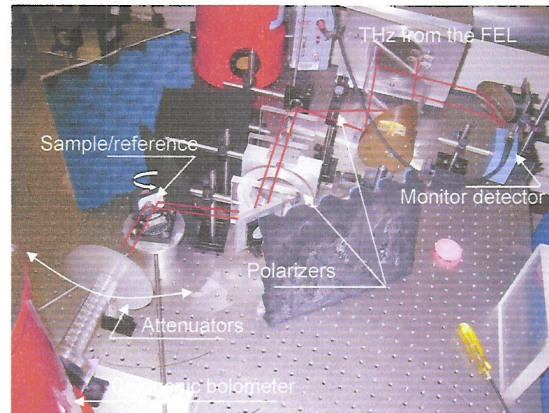


Fig. 9 Apparatus to measure reflectivity versus take off angle using radiation from the free-electron lasers.

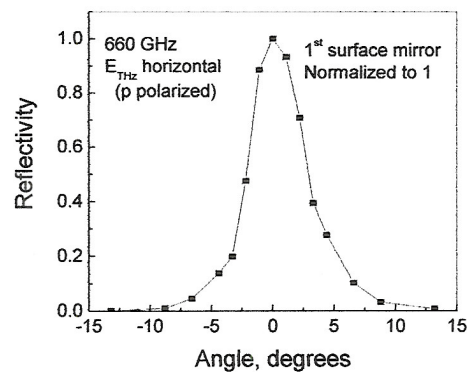


Fig. 10 Reflectivity versus angle for 1st surface mirror used as a reference. Angle of incidence ~ 45°.

Fig. 11 shows the angular dependence of the reflectivity for the rough surface for the four combinations of polarization and orientation of the sander induced striations. *The wild structure is almost certainly not interesting, most likely due to interference between the reflected radiation and spurious reflections from other parts of the setup at these relatively long wavelengths (~ 0.5 mm).* Note that the reflectivity from the sample drops to ~ 0.2 and ~ 0.03 for s and p polarization respectively, and the spurious reflections become a larger and more important fraction of the total signal. Future work will mitigate these effects.

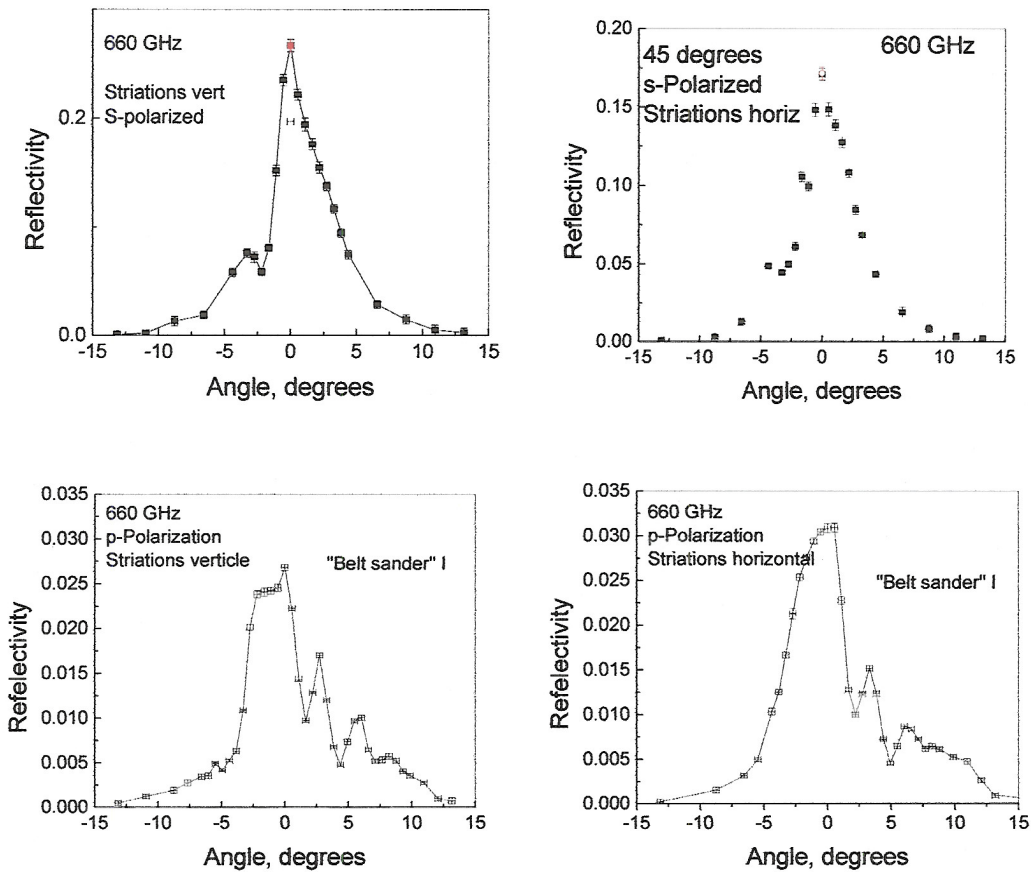


Fig. 11 Reflectivity normalized to a first surface mirror. S and p polarizations, with striations introduced by “belt sanding” this pellet, oriented horizontal, parallel to the plane of incidence, or vertical, perpendicular to the plane of incidence. The structure is experimental artifact introduced by spurious radiation, multi path, which destructively and constructively interferes with the main reflected signal. It is more problematic at lower measured sample reflectivity. *Future work will mitigate these effects.*

The systematic errors introduced by the multi-path effects notwithstanding, we can estimate the reflectivity for these two polarizations and project the results on a simple dielectric model for this material. At 45° the reflectivity from a single dielectric interface can be calculated as a function of dielectric constant or index of refraction, n. At 45° $R_p = R_s^2$.

The calculated s and p polarized reflectivity at 45 ° vs index is displayed in Fig. 12. Admitting considerable uncertainty in the measured reflectivity introduced by multi-path interference, we can estimate that the index of refraction at 660 GHz is ~1.85.

Near normal reflectance 600GHz, at the diffraction limit

We reexamined the reflectivity from the simulant at near normal incidence (angle of incidence of $\sim 3.5^\circ$) with higher angular resolution, mitigating to some extent the multipath effects on the reflectivity. The experimental setup, shown in Fig. 13 was used at 600 GHz to measure the reflectivity of both the rough and polished surfaces with various orientations of the surface striations and incident terahertz electric fields.

Preliminary results at 600 GHz indicate that at this angular resolution, which is set largely by diffraction but with significant but subordinate contribution from the instrument, the effect of roughness of the pellet at 600GHz is not significant. The results are displayed as a composite in Fig. 14. Data are normalized to 1. The reflectivity from the simulant was roughly 0.1 and consistent with other measures at this frequency. The solid line is a gaussian with a width determined by diffraction from the target and angular resolution set by the instrument geometries.

It is possible, but not tested at this time, that there is scattering or reflection at larger angles, in the wings, that is sensitive to roughness of the surface. This is left to future work. On the other hand the reflectivity around the specular angle does not depend on roughness so one may conclude that the large angle diffuse components are small.

It is also instructive to compare these results with the frequency dependent, near normal,

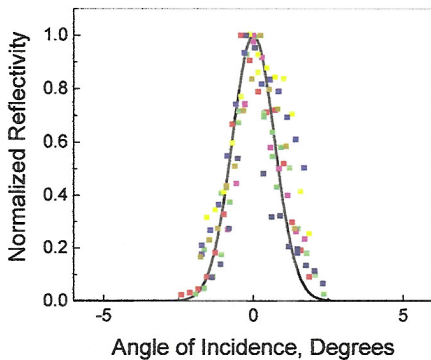


Fig. 14 Normalized reflectivity versus angle for various surfaces. (See text.) Solid line depicts instrumental resolution as a Gaussian including diffraction.

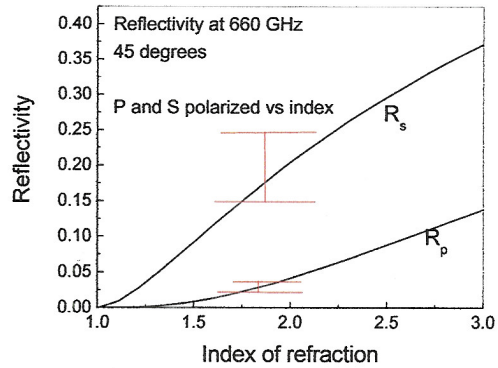


Fig. 12 Reflectivity at 45 degrees versus index of refraction.

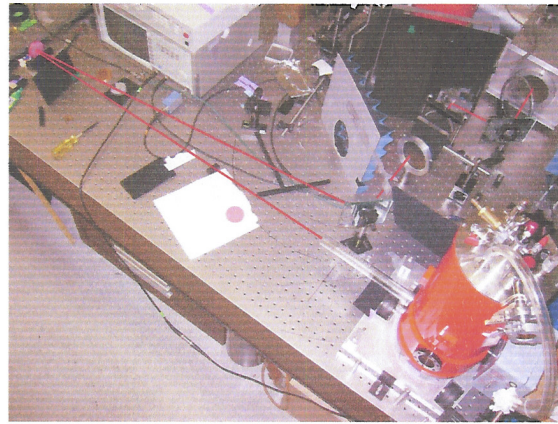


Fig. 13 To mitigate multipath and gain higher angular resolution terahertz transport was simplified and reoriented to explore near normal reflectivity.

reflectivity obtained from the same surfaces with the FTIR instrument shown in Fig. 2. There is little discernible difference between the rough and polished surfaces below 1 THz, whereas the measured reflectivity at 3 THz, $\sim 100 \mu\text{m}$ wavelength, is strongly affected by the surface roughness. The FTIR reflectometer senses the specular component. Presumably the reduction in specular reflectivity at 3 THz is accompanied by increased diffuse scattering.

Real targets with surfaces like those presented by the simulant will be highly specular. Attempts to gain spectral information may be compromised if

the return signal is dominated by those target features that happen to present specular reflection back to the THz detector, receiver or THz focal plane array.

Transmission through the Simulant.

Reflectivity measurements are more complicated to interpret if the material is transparent. Under these conditions the reflected signal will also come from the second surface: Fabry-Perot resonances may also produce structure in the spectrum of reflected radiation.

Fig. 15 displays the normal incidence transmission versus frequency for the simulant along with the reflectivity at 45° for various orientations of the THz electric field and belt sander induced surface striations. It is apparent that the simulant becomes more transparent as the frequency approaches 300-400 GHz. An analysis of the transmission and reflection including Fabry-Perot resonances is not available at this time.

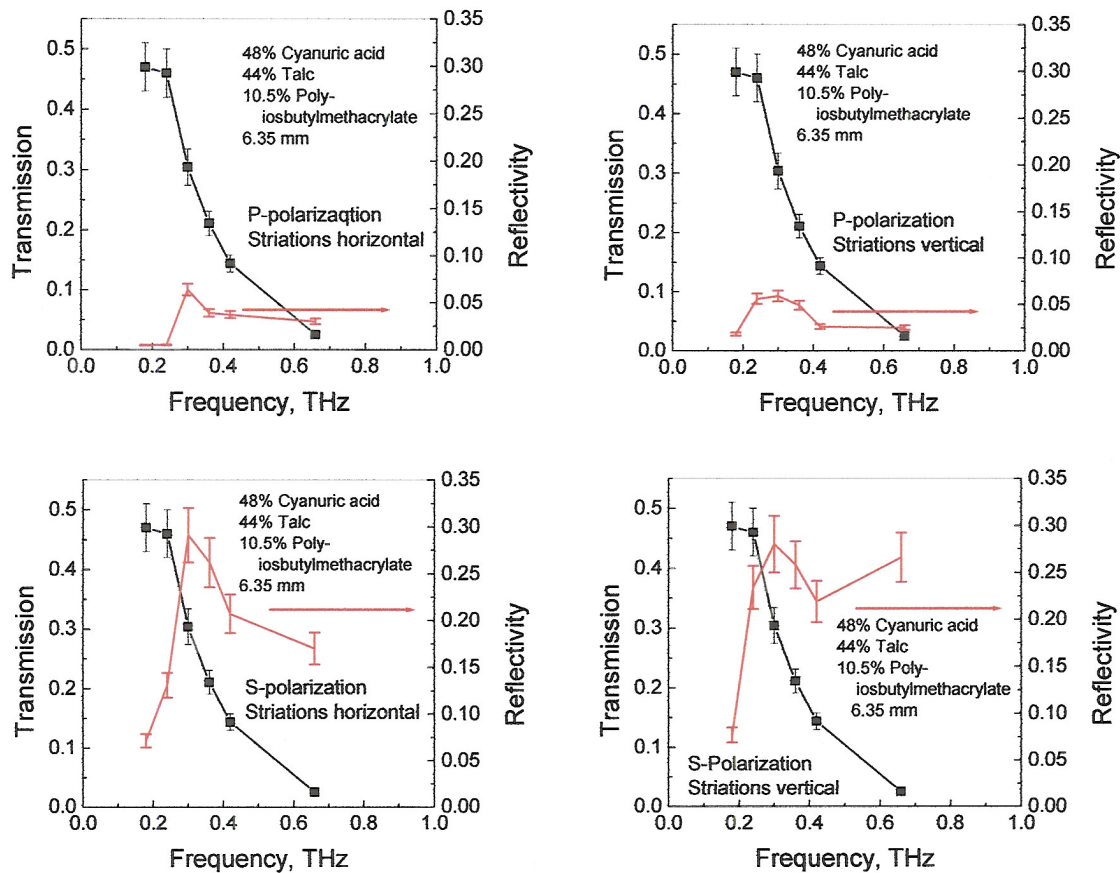


Fig. 15 Transmission at normal incidence vs frequency, superimposed on reflectivity versus frequency at 45° for various orientations of the THz electric vector and surface striations.

We do note that all highly disordered materials (the simulant is a disordered composite), which contain polarizable constituents, exhibit absorption that increases strongly with THz frequency. Conventional wisdom explains that disorder breaks any selection rules and allows the nearly spatially uniform THz field to couple to all available modes through any polarizability. The density of modes, at THz frequencies, increases quadratically with frequency.

Terahertz Transmission through Various Materials

Stand off detection of high explosives requires terahertz spectroscopic imaging of targets over some distance through the atmosphere and through various materials that may hide the high explosives. Material carried by a suicide bomber would most likely be masked by clothing or carrier like a knap sack.

Atmospheric water

Fig. 16 shows the nominal atmospheric absorption primarily due to water vapor up to 3 THz. The path length is total path length. That is to say, a target at 5 meters requires a technology that sees through 10 meters of atmosphere shown in the figure. Water vapor absorption rapidly limits technology to low terahertz frequencies as distance increases.

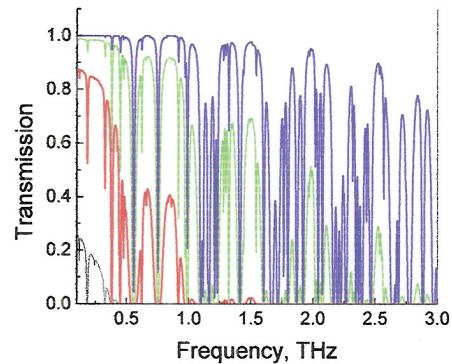


Fig. 16 Nominal transmission through the atmosphere with total path length as a parameter. 1, 10, 100, 1000 meters as blue, green, red, black. Stand off interrogation at 5 meter would experience the attenuation shown for 10 meters. [1]

Miscellaneous fiber materials, some clothing related.

During the contract period the transmission through several fabrics were investigated. In the spirit of the potential application, the reflectivity of the polished brass reference mirror, uncovered and covered with various materials, was measured with the FTIR spectrometer. The signal recovered represents the terahertz radiation reflected by the brass after passing through two thicknesses plus any radiation directly reflected by the material draped over the reflector. There is little or no detected baseline at high frequencies where the transmission appears to be vanishingly small and we suspect there is no significant contamination from reflectivity from the fabric itself.

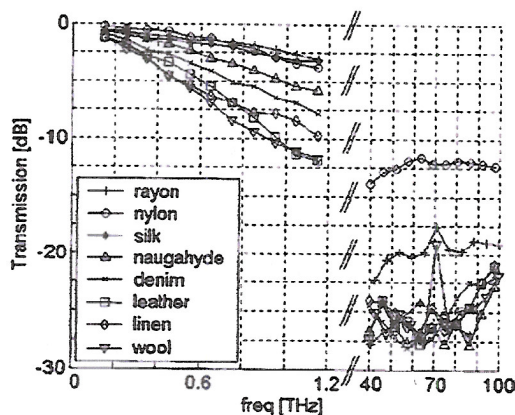


Fig. 18 Transmission through various materials. J. E. Bjarnason, et al 2

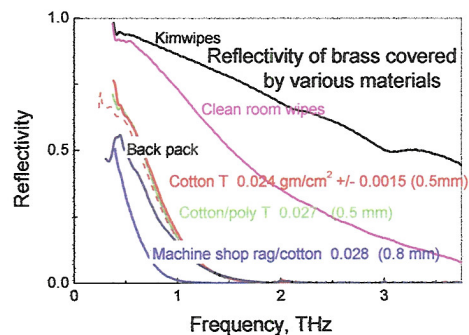


Fig. 17 Reflectivity of brass reference mirror covered by various materials, normalized by the brass reference reflector itself. Note that the back pack material was rubber backed canvas.

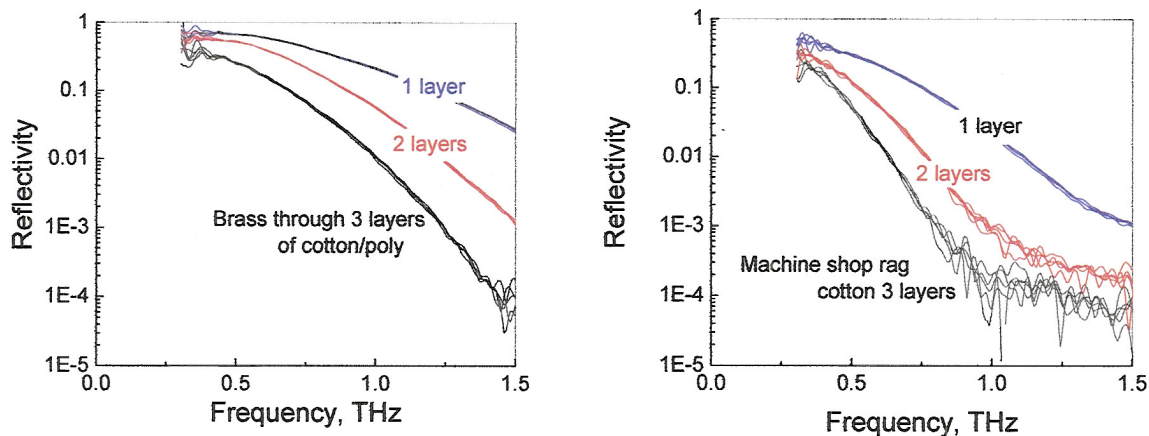


Fig. 19 Reflectivity of brass reference mirror after transmission of terahertz radiation through various thicknesses of cotton fabric. See 2. Right: Open textured commercial machine shop rag made of Pakistan cotton. Left: Cotton polyester blend, tight weave.

Consultation with LLNL staff provoked a more careful examination of the data presented in Fig. 17. Displaying the data on a plot of log reflectivity vs frequency exposes the transmission behavior at high frequencies, where the material appears opaque in Fig. 17. The data is displayed as several (5) overlapping traces to provide the reader with a sense of reproducibility. There are no sharp features that deserve special attention. The cotton/polyester blend roughly scales correctly. The open weave commercial machine shop rag does not. An explanation is not offered.

Careful examination of Fig. 17 reveals that the transmission through the cotton fabrics may not be simply controlled by the amount of material in the beam as measured by the weight. The cotton, cotton poly blend have the same weight per area and exhibit the same attenuation vs frequency. The open weave, machine shop cotton rag (clean, unused) has the same weight per area but stronger attenuation. Perhaps, the attenuation is caused as much by scattering as absorption. (The measurements shown in Fig. 17 do not distinguish diffuse scattering from attenuation.) The machine shop rag is noticeably courser.

On the other hand diffuse scattering from covering fabric may be an advantage. Terahertz spectroscopic imaging system requirements will be quite different if the return radiation is specular or it is diffuse. *Perhaps a target that presents specular surfaces when naked will appear diffuse when covered with fabrics.*

This data sample is limited but indicates that identification of threatening materials by terahertz spectroscopic imaging is compromised at frequencies above 1 THz by any sort of cover. We also include for reference recent work published by E.R. Brown and coworkers that addresses the same issue (Fig. 18).[2]

1 HITRAN 1996 data base, Ontar Corporation.

2 “Millimeter-wave, terahertz, and mid-infrared transmission through common clothing”, J. E. Bjarnason, T. L. J. Chan, A. W. M. Lee, M. A. Celis, and E. R. Brown, *Appl. Phys. Lett.*, **85**, 519 (2004).